JOTCSB Journal of the Turkish Chemical Society Section: B Chemical Engineering
TURKISH CHEMICAL SOCIETY

Ultimate Eradication of Acid Orange 7 from Contaminated Liquid via Synthesized Mesoporous Goethite

Davoud Balarak[1], Fatemeh Ganji[2], Periakaruppan Rajiv[3], Chinenye Adaobi Igwegbe[4]*, Joshua O. Ighalo[4,5]

[1]Department of Environmental Health, Health Promotion Research Center, Zahedan, University of Medical Sciences, Zahedan, Iran.
[2]Student Research Committee, Zahedan University of Medical Sciences, Zahedan, Iran.
[3]Department of Biotechnology, Karpagam Academy of Higher Education, Eachanari Post, Coimbatore 641 021, Tamil Nadu, India.
[4]Department of Chemical Engineering, Nnamdi Azikiwe University, P.M.B. 5025, Awka, Nigeria.
[5]Department of Chemical Engineering, University of Ilorin, P. M. B. 1515, Ilorin, Nigeria.

Abstract: This paper carried out the study on the adsorption of Acid Orange 7 (ACO7) from aqueous solutions by mesoporous goethite (MPG). The adsorbent was characterized by XRD, FE-SEM, BJH desorption, and BET. The effect of process variables such as MPG dosage, reaction time, concentration of ACO7, pH, and reaction temperature on the ACO7 uptake capacity were systematically investigated in an attempt to illustrate adsorption performance of MPG. Optimal condition for the adsorption process was 1 g/L adsorbent dosage, temperature of 328 K, pH of 3, 75 minutes' contact time and 100 mg/L ACO7 concentration which yielded a removal efficiency of 90.13%. The adsorption kinetic was best fit to the intra-particle diffusion model while the equilibrium isotherm was best fit to the Langmuir model, suggesting that homogeneous uptake was the principal mechanism adopted in the process of ACO7 adsorption with a monolayer adsorption capacity, q_m of 117.9 mg/g. The study revealed that the pseudo-second order model and the Langmuir isotherm model were the best-fit kinetics and isotherm models to describe the process. The uptake of ACO7 by MPG was endothermic and spontaneous. The major mechanisms for ACO7 uptake onto MPG were pore diffusion, hydrogen bonds, π – π stacking interactions and hydrophobic interactions. MPG has excellent reusability potential with only an 8% drop in performance after 8 cycles. These results indicate that MPG has wide application prospects in removing ACO7 from wastewater.

Keywords: Acid Orange 7, Adsorption, Dye, Goethite, Water Pollution

Submitted: January 23, 2021. **Accepted:** March 01, 2021.

Cite this: Balarak D, Ganji F, Rajiv P, Igwegbe CA, Ighalo JO. Ultimate Eradication of Acid Orange 7 from Contaminated Liquid via Synthesized Mesoporous Goethite. JOTCSB. 2021;4(1):13–26.

***Corresponding author. Email:** ca.igwegbe@unizik.edu.ng

INTRODUCTION

Dyes are used all over the world for miscellaneous purposes (1, 2). Colorizing the industrial products of textile, paper, printing leather, food and cosmetic produce large amounts of colored wastewater (3-5). Pulp, paper, and textile industries have been considered as major polluting units across the world (6-8).

Industrial dyes are the main sources of environmental pollution due to their high-toxicity, non-biodegradability, mutagenic, and carcinogenic characteristics (9, 10). Effluent containing dyes should be treated before it is discharged to the environment due to its toxicity (11, 12). Hence, there is an immense interest in the uptake of dyes from polluted water using non-toxic, cost-effective and biodegradable materials (13, 14). Acid Orange 7 (2-naphthol orange or Orange II) is an inexpensive and moderately fast azo dye (15, 16). Its popular use and regular occurrence in effluents (17) was the reason it was selected for the current study.

With the increasing public concerns on environmental protection, removal of colorful

dyestuffs from wastewater has become an especially important issue (18, 19). Dye removal can be managed via coagulation, biodegradation, chemical degradation, and photo-degradation and adsorption methods (20). Every method has advantageous and disadvantageous from the points of effectiveness and cost except adsorption (20, 21). In recent years, adsorption method with low cost, high operability and no secondary pollution has been widely used to remove dyes in aqueous environments and soils (12, 21). There are a lot of investigations about the utilization of renewable and low budget adsorbents like *Azolla filiculides*, *Lemna minor*, Canola, pumice stone, bentonite, cherry kernels, husk rice, sewage sludge and montmorillonite (22-24).

Goethite is an environmental stable iron oxy-hydroxide (25). Researchers have employed it for water management (26, 27). The study on the capacity of adsorption of goethite is scarce (28, 29). The utilization of mesoporous goethite (MPG) for the adsorptive uptake of pollutant dye like Acid Orange 7 (ACO7) is unreported, therefore, this study was done. The adsorption capacity of MPG for ACO7 uptake from liquid was examined. The characterization of MPG was done via the X-Ray Diffraction (XRD), Field Emission Scanning Electron. Microscopy (FE-SEM), Barrett-Joyner-Halenda (BJH) desorption and Brunauer-Emmett-Teller (BET). The effects of several process elements such as MPG dose, pH, time of contact, ACO7 concentration, and temperature on adsorbate uptake was examined. This study also considered the adsorption kinetics, isotherms, thermodynamics and mechanism of the adsorption process.

EXPERIMENTAL SECTION

Reagents

Acid Orange 7 (2-naphthol orange or Orange II) is an azo dye (molecular formula:$C_{16}H_{11}N_2NaO_4S$, molecular mass:350.32g/mol). The molecular structure of the ACO7 has been represented in Figure 1. Ferrous sulfate heptahydrate, Acid Orange 7, hydrogen peroxide (30%), sodium hydroxide, and hydrochloric acid were obtained from Sigma Aldrich. A stock solution of ACO7 (500 mg/L) was synthesized through suspending a suitable measurement of the ACO7 in ultrapure-water. All reagents used in the study were of analytical grade.

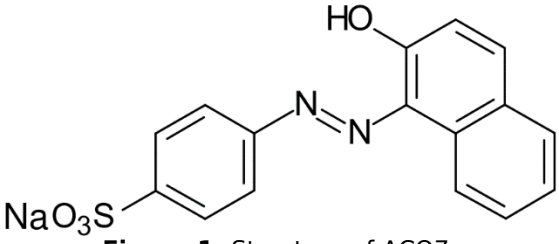

Figure 1: Structure of ACO7.

MPG preparation

The MPG was synthesized using the procedure reported by (**See supplementary**). The characterization of MPG was done via the XRD, FE-SEM, BJH desorption and BET.

Batch adsorption studies

The effect of process factors such as MPG dose, time of contact, initial ACO7 concentration, pH and temperature was considered during a batch process. The temperature of the batch adsorption experiment was varied at 10, 25, 40 and 55 °C; and the removal of ACO7 was performed as described above. The effect of contact time was evaluated through measurements 10, 20, 30, 45, 60, 90 and 120 min. Each experiment was done using a 100 mL solution of the dye having a specified initial concentration. The pH of the dye solution was adjusted using 0.1 N HCl or NaOH. A known quantity of MPG was introduced into the ACO7 solution and magnetically stirred at 160 rpm for a given period. When the contact time is achieved, the solution is filtered out by Whatman filter paper. Dye concentrations were analyzed using UV/VIS spectrophotometry (Shimadzu, Japan; Model DR 5000) at λ_{max} = 484 nm. The ACO7 adsorbed on MPG was evaluated using Eq. 1 (30):

$$q_e = \frac{(C_0 - C_e)V}{m} \quad \text{Eq. 1}$$

Where C_0 (mg/L) is the initial ACO7 concentration, *Ce* (mg/L) is the ACO7 concentration at a specific time, *V* (m^3) is the volume of ACO7 solution, and *M* (g) is the MPG amount, respectively.

The % removal efficiency is determined using Eq. 2 (31). The dimensionless separation factors (R_L) is determined using Eq. 3 (32), where K_L is the Langmuir constant.

$$R_e(\%) = \frac{(C_0 - C_e)}{C_0} \times 100 \quad \text{Eq. 2}$$

$$R_L = \frac{1}{1 + K_L C_0} \quad \text{Eq. 3}$$

RESULTS AND DISCUSSION

Characterization of MPG

XRD analysis was done through an X-ray diffractometer with Philips PNA-analytical diffractometer. Figures 2-3 shows the characterization of MPG. The MPG reveals typical characteristic peaks (Figure 2) at 19.44°, 33.09°, 36.75°, 44.64°, 59.71° and 66.97°, corresponding to 110, 130, 111, 140, 151 and 061 of MPG (JCPDS no. 29-0713), respectively. The sharp and intense MPG peaks suggest that the material is crystalline in nature (33). FE-SEM experiment was carried out using a scanning electron microscopy (SEM) (JEOL, JSM 6500F). FE-SEM image shown in Figure 3 reveals the presence of spherical clusters, but most agglomerated. The heterogeneous outlook suggests the MPG have good surface area and applicable as a

sorbent (34). The N_2 adsorption isotherm was obtained by means of Quantachrom ChemBET-3000 USA. N_2 adsorption-desorption isotherms and BJH desorption of goethite and MPG is shown in Figure 4. The adsorption-desorption isotherm curves of MPG exhibit a type IV isotherm with H3 hysteresis loop which reveals that the adsorbent has a mesoporous nature. However, the adsorption-desorption isotherm curves of goethite reveal a type III isotherm and the hysteresis loop becomes inconspicuous, indicating no typical pores appearance (29). The specific surface area of MPG and common goethite are 194.35 and 149.64 m^2/g, respectively. It can be observed that the synthesized MPG has a greater surface area than goethite. Specific surface area is an important property of an adsorbent as it affects the sorbate-sorbent interface and influences the extent of adsorbate uptake (35).

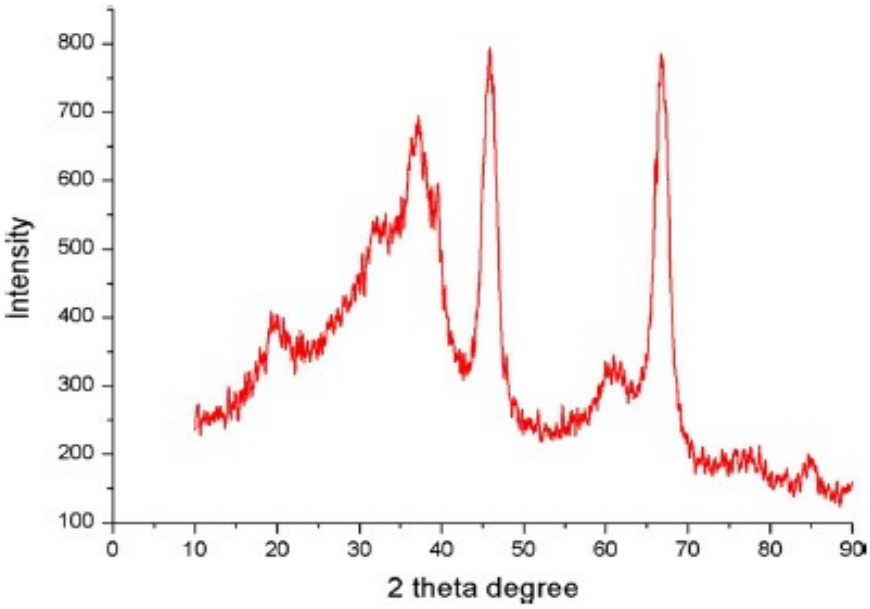

Figure 2: The XRD of MPG.

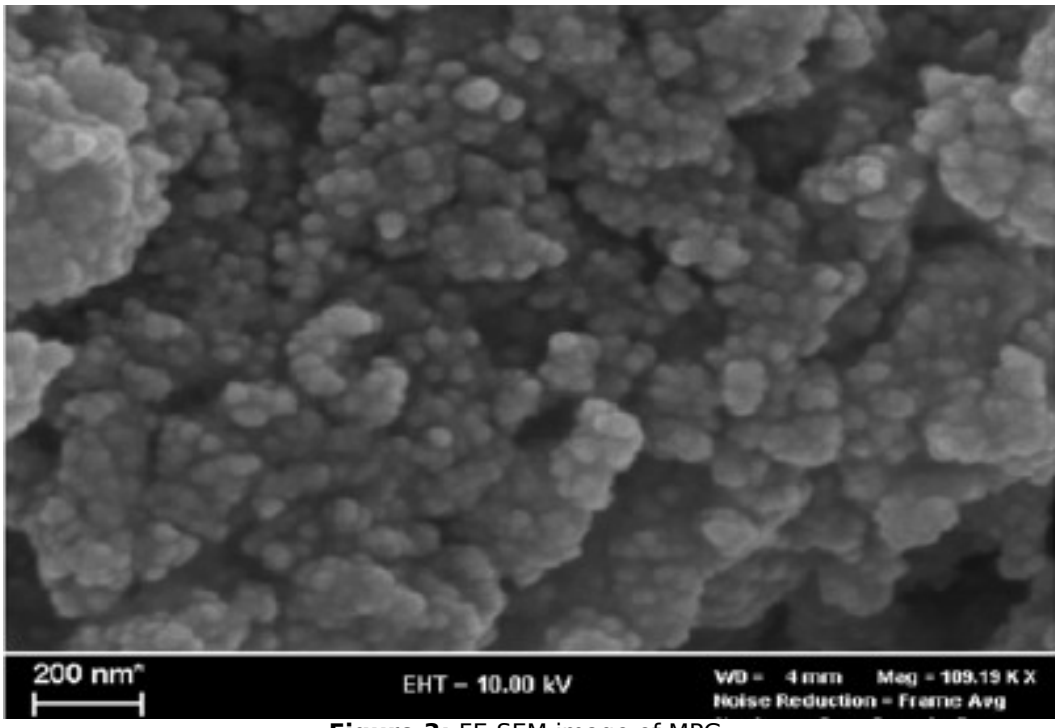

Figure 3: FE-SEM image of MPG.

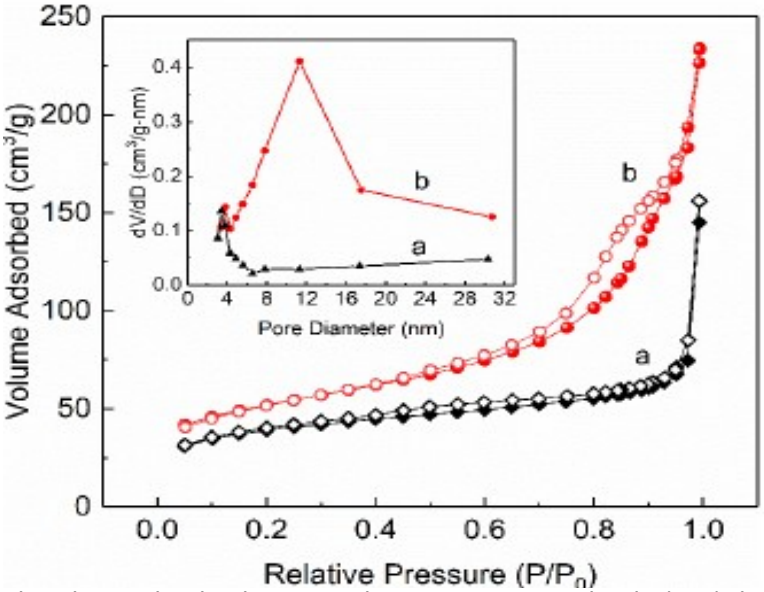

Figure 4: N_2 adsorption-desorption isotherms and Barrett-Joyner-Halenda (BJH) desorption of goethite (a) MPG (b).

Effect of process factors

Impact of pH

The impact of pH on ACO7 removal was inspected at a contact time of 75 min, MPG dose of 1 g/L, initial ACO7 concentration of 100 mg/L and at 25± 2 °C. The pH was studied between 3–11. As shown in Figure 5, the amount of ACO7 removal decreased from 90.88 to 48.45%, when pH changed from 3.0 to 11.0. In contrast, at a higher pH, the aggregation of the zwitterionic form of ACO7 molecules occurs leading to electrostatic interactions between the carboxyl groups on the MPG (36). This aggregation of ACO7 leads to the formation of large ACO7 dimers that are then unable to penetrate the MPG, decreasing the adsorptive removal of ACO7 (37). In acidic pH values, the adsorbent surface has a net positive charge, and a complexation occurs between the positive charges of adsorbent and the negative ions of the dye (36). It demonstrates the ability to compete between -OH ions in dye with available and active sites at the adsorbent surface (26). The optimum pH was at 3 and this was utilized for other experiments.

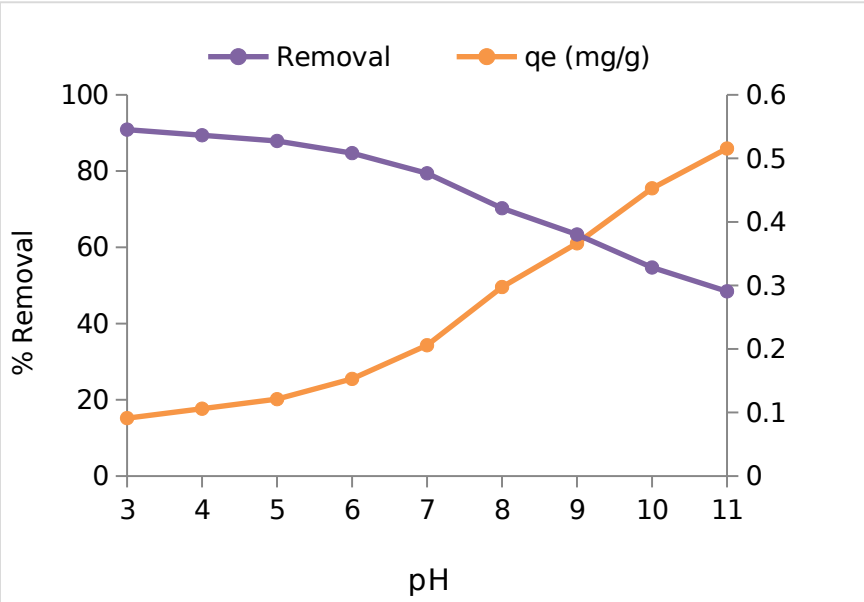

Figure 5: Impact of pH on ACO7 removal (at time =75 min, MPG dose = 1 g/L, C_0 = 100 mg/L, temp = 25 °C).

MPG dose effect

The effect of MPG dose on ACO7 removal was investigated at 25± 2 °C. As shown in Figure 6, the effect of dosage on MPG adsorbed ACO7 was studied with doses of the range 0.2 - 1.4 g/L. The adsorption ratio increased rapidly as MPG dose

increased and the adsorption ratio was not increased considerably when MPG doses were higher than 0.6 g/L. When the dosage of MPG was about 1 g/L, the adsorption ratio of ACO7 reached the maximum (90.88%). Increasing the dosage of MPG, the adsorption sites of adsorbent could not be full-scaled used and made some adsorption sites approached so that the adsorption capacity of the ACO7 per unit of MPG gradually reduced (38). In general, the dosage of MPG affects the surface area and the available active sites (39). The optimal MPG dosage was 1 g/L and this was used for the rest of the experiments.

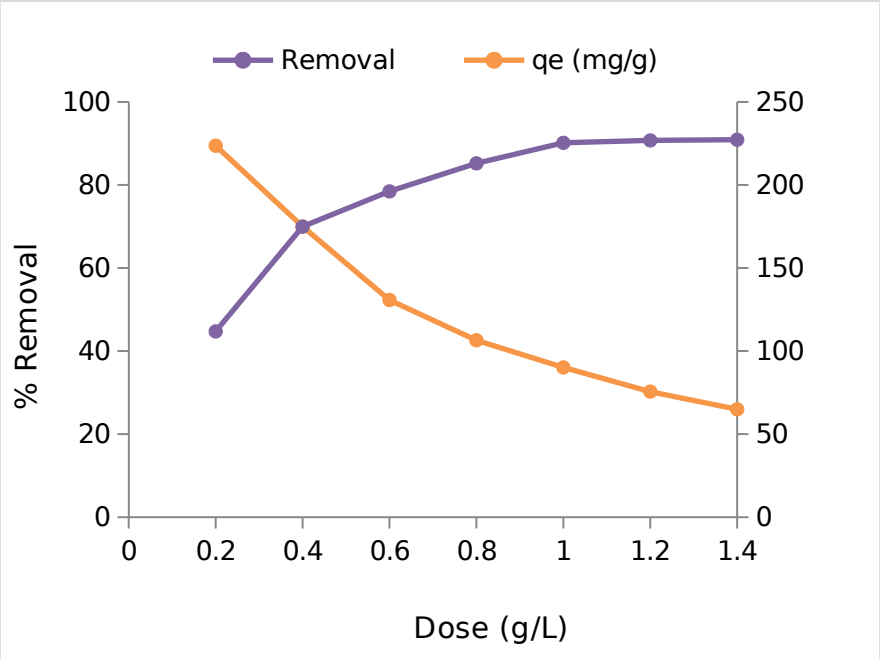

Figure 6: Effect of MPG mass on ACO7 adsorption (at C_0 = 100 mg/L, temp = 25 °C, time = 75 min, pH = 3).

Impact of temperature

The investigation of temperature effect on the uptake of ACO7 was done by measurements at 10, 25, 40 and 55 °C (Figure 7). The results showed that ACO7 uptake on MPG was improved with elevating temperature. With increasing temperature, the mobility of dye molecules increases, which can facilitate penetration to surface/interface of adsorbent (40-41). This showed that the process was endothermic which was also confirmed by the thermodynamics modeling results, and the increasing temperature was beneficial to the adsorption of ACO7 on MPG. The result was similar to those reported by some researchers (33, 42). Another hypothesis was that as the temperature increases, the approached sites, structure and volume of the pores on the surface of the adsorbent were increased, which enhanced the relevant adsorption properties of the MPG adsorbents (43).

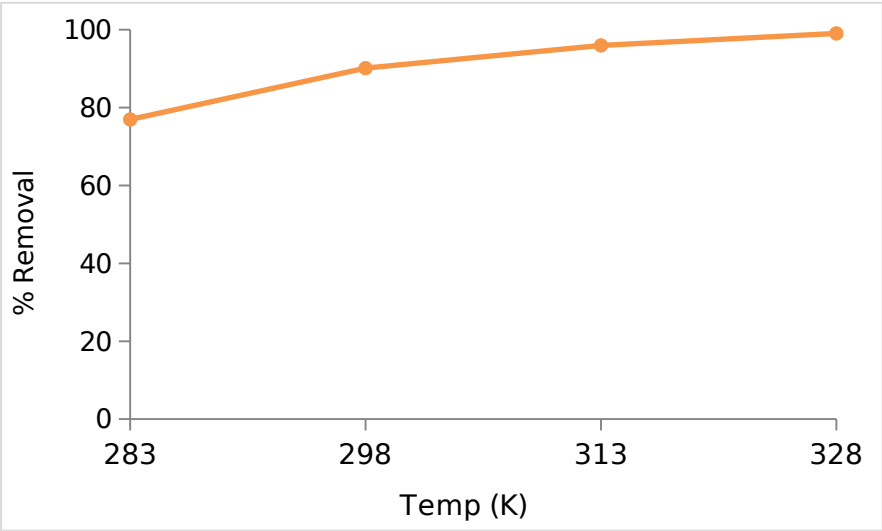

Figure 7: Impact of adsorption temperature on ACO7 removal (at C_0 = 100 mg/L, MPG dose = 1 g/L, time = 75 min, pH = 3).

Impact of ACO7 concentration and contact time

The adsorptive uptake was rapidly increasing at the commencement of the adsorption process and gradually reduced as the adsorption progressed towards equilibrium (Figure 8). This was because the amount of the dyes in the solution was high at the start of experiments, and there were still much-unoccupied adsorption sites of MPG (44). High initial concentration also favored the adsorptive uptake of ACO7 because it leads to a greater mass transfer driving force of the adsorbate across the sorbate-sorbent liquid film (45, 46). Equilibrium was achieved after about 75 minutes. As the adsorption proceeding, the decreasing adsorption rate gradually decreased due to the adsorption sites were gradually occupied by contaminants (47).

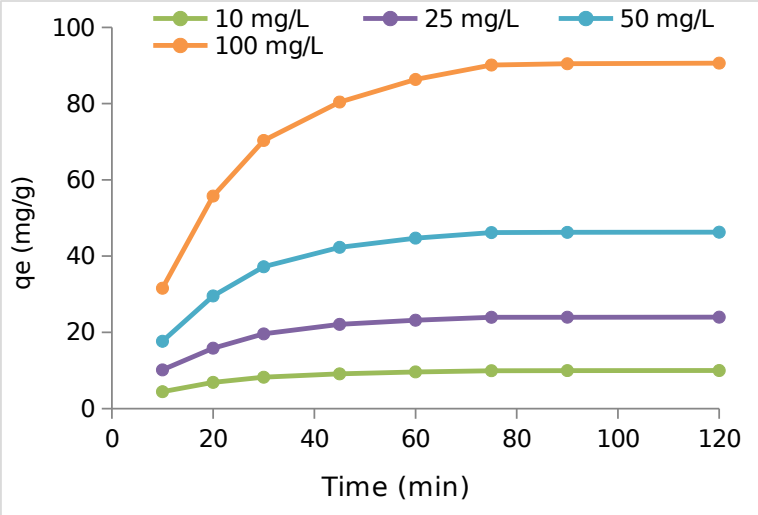

Figure 8: Effect of ACO7 concentration and time on ACO7 uptake (at MPG dosage = 1 g/L, pH = 3.0, temp = 25 °C).

Adsorption isotherm modeling

The adsorption of ACO7 onto MPG was modeled using the Langmuir (48), Freundlich (49), Temkin (50) and Dubinin–Radushkevich (D-R) (51) isotherms. From Table 1, the Langmuir isotherm model was observed to be best-fit for the adsorption data based on the closeness of the R^2 values to 1. The values of the separation factor (K_L) showed an increasing trend with temperature increase. This suggests that ACO7 adsorption is an endothermic process and this is confirmed by the thermodynamics result. Since the K_L values are less than 1, it also shows that the adsorption process is favorable. The good adaptability of Langmuir isotherm to experimental data means that homogeneous surface exists in MPG and that the adsorption of ACO7 onto MPG takes place as a monolayer (52). The monolayer adsorption capacity of ACO7 onto MPG is 117.9 mg/g (at 328 K).

The K_F values of the Freundlich isotherm was in the range of 4.72~9.14 and it showed an increasing trend with temperature increase, again confirming the endothermic nature of ACO7 uptake by MPG. The values of 1/n were also found in the range of 0.141~0.279 at all temperatures used, signifying again that adsorption is favorable. The Temkin isotherm model parameters K_T and B_T increased with temperature which indicates that the heat of adsorption of ACO7 onto the surface of MPG is endothermic. From the D-R isotherm, the values of E were found all smaller than 16 kJ/mol (Table 1), suggesting that the sorption type of ACO7 onto MPG was majorly by physical mechanisms.

Table 1: Isotherm parameters for adsorption of ACO7 onto MPG at various temperatures.

Temp (K)	Freundlich			Langmuir			
	K_F	1/n	R^2	q_m	R_L	K_L	R^2
283	4.721	0.141	0.814	90.62	0.441	0.0127	0.992
298	6.194	0.185	0.849	97.25	0.337	0.0196	0.995
313	7.962	0.224	0.879	106.4	0.281	0.0256	0.998
328	9.147	0.279	0.825	117.9	0.226	0.0342	0.991
Temp (K)	**Temkin**			**D-R**			
	B	K_T	R^2	q_s	**E**		R^2
283	7.42	0.112	0.918	45.69	0.425		0.904
298	8.73	0.195	0.895	51.25	0.691		0.925
313	9.13	0.264	0.927	56.74	0.819		0.896
328	9.87	0.371	0.943	63.79	1.054		0.941

Kinetics modeling

The kinetics of the adsorption of ACO7 onto MPG was modeled by the pseudo-first order (53), pseudo-second order (54) and intra-particle diffusion (55) models. The results are summarized in Table 2. From the table, it can be observed that the intra-particle diffusion model is the best fit for describing the adsorption process due to its high coefficient of determination (R^2) values. The intra-particle diffusion model proceeds in two steps hence the results shown in Table 2 are for step 1 and 2. In the first step, the uptake of ACO7 occurred on the surface of adsorbents, while in the second step, the adsorbate penetrates through the pores of the adsorbents (56). The values of K_1, and K_2 are the rate parameters for the first step and second step respectively. The R2 vales of the IPD step is higher which suggests that the adsorption takes place majorly on the surface. From modeling itself, it was observed that the intercept was not equal to zero, this explained that intra-particle diffusion was not the only rate-controlling step in the adsorption process. The pseudo-second order model was also well fitted to the adsorption data with similar conclusions obtained by previous research (57, 58). This is suggestive that both the amount of available MPG active sites and the concentration of ACO7 adsorbate in the aqueous phase affects the adsorption process (59).

Thermodynamics modeling

Thermodynamics modeling was done to determine the value of some of the parameters, like the change in enthalpy (ΔH°), Gibbs energy (ΔG°) and entropy (ΔS°) for the adsorption of ACO7 on MPG were calculated at different temperatures using Eq. 4-5 (10)

$$\Delta G° = - RT \text{ Ln } K \qquad \text{Eq. 4}$$

$$\ln K = \frac{\Delta S^0}{R} - \frac{\Delta H^0}{RT} \qquad \text{Eq. 5}$$

The values of ΔH°, ΔG° and ΔS° parameters obtained from the modeling are summarized in Table 3. The negative values of ΔG° suggest ACO7 uptake by MPG is spontaneous and the greater the negative value of ΔG° goes, the more energetically favorable the adsorption becomes (60). The enthalpy change (ΔH°) was +57.58 KJ/mol, therefore, ACO7 uptake by MPG is an endothermic process (43). Also, the positive value of entropy change (ΔS°= +0.212 KJ/mol·K) indicates that the randomness of the solid-solution interface increases during the adsorption of the ACO7 to the MPG (61, 62). The small magnitude of the values of ΔG° (<20 KJ/mol) suggest that the uptake of ACO7 onto MPG is by a physical mechanism (63).

Adsorption mechanism

To gain a proper understanding of the nature of the adsorption process, it is important to conduct a holistic mechanistic analysis (35). Based on the isotherm and thermodynamics modeling studies, it is surmised that physical interactions are the major uptake mechanism of ACO7 onto MPG. At optimal pH (3.0), there is complexation between Fe cations on the MPG surface and the ACO7 adsorbate. These coordination surface complexes are formed by coordinate covalent interactions between the ligands (ACO7 in this case) and the metallic ions (Fe cations). This is achievable because ACO7 has acid dissociation constants of 11.4 (pK_{a1}) and 1.0 (pK_{a2}) (64) hence has valence electrons at the optimum pH (3.0).

However, since physical interaction forces are more significant at these optimum conditions, the presence of Van der Waals' forces are also responsible for much of the uptake (65). This is due to hydrogen bonds between –OH on goethite and the hydrogen atoms on the adsorbent. Furthermore, at the zwitterionic form of the adsorbent, the solubility is usually low and the hydrophobic effect of the surrounding aqueous phase increases the adsorptive uptake as the ACO7 then possesses a greater affinity for the solid phase (MPG in this case).

Based on the kinetic modeling, it is also observed that pore diffusion is another important mechanism of ACO7 uptake onto MPG. From Figure 1, the multiple benzene rings in ACO7 shows it is a polycyclic aromatic compound. These benzene rings possess electron-rich zones around the carbon atoms that could induce a stacking effect on the adsorbent. Such π – π stacking interactions are an important mechanism of uptake for the adsorption process. The different mechanisms for ACO7 uptake onto MPG are surface complexation, hydrogen bonds, pore diffusion, hydrophobic interactions, and π – π stacking interactions and these are summarized in Figure 9.

Comparison with other adsorbents

In this section, the adsorption capacity of other adsorbents for ACO7 uptake was compared with that of MPG. The findings are summarized in Table 4 to four significant figures and sorted in decreasing order. It was also important to report the pH and temperature at which these were achieved because they are relevant factors that affect the adsorption process. It can be observed that MPG have intermediate adsorption capacity in comparison with other adsorbents reported in literature. It is also observed that for most adsorbents, a low pH is required for the effective performance of the adsorbent. The implication in sustainable water management is in pre-acidification of effluent before adsorptive treatment.

Table 2: Summary of kinetics modelling for ACO7 onto MPG

C_o (mg/L)	q_e exp (mg/g)	PFO			PSO			IPD (step 1)			IPD (step 2)		
		K_1	q_e	R^2	K_2	I	R^2	K_1	q_e	R^2	K_2	I	R^2
10	9.71	0.073	3.72	0.841	0.051	1.951	0.859	0.721	0.211	0.956	0.051	1.951	0.859
25	23.67	0.059	9.14	0.872	0.098	2.762	0.872	0.941	0.495	0.942	0.098	2.762	0.872
50	46.28	0.061	23.73	0.804	1.091	4.826	0.884	1.452	0.652	0.935	1.091	4.826	0.884
100	90.62	0.043	45.84	0.897	1.273	5.839	0.865	1.872	0.841	0.948	1.273	5.839	0.865

PFO – Pseudo-first order, PSO – Pseudo-second order, IPD – Intra-particle diffusion

Table 3: Values of thermodynamic parameters for the adsorption of ACO7 onto MPG.

Temp (K)	ΔG^0 (KJ/mol)	ΔH^0 (KJ/mol)	ΔS^0 (KJ/mol K)
283	-2.83		
298	-5.47	57.58	0.212
313	-8.24		
328	-12.64		

Table 4: Comparison of sorbent performance for ACO7 uptake

Adsorbents	Temp (K)	pH	q_m (mg/g)	Ref.
AC from spent coffee/calcium-alginate beads	303	3.0	665.9	(64)
Mg-Al layered double hydroxide	298	-	485.6	(66)
Amberlite FPA-98	303	7.0	200.0	(15)
MPG	**328**	**3.0**	**117.9**	**This study**
MWCNT	298	7.0	47.72	(67)
Kenya tea pulps ash	-	2.0	41.66	(68)
ZnO nanoparticles	298	3.0	32.13	(69)
Spent brewery grains	303	4.5	30.50	(70)
Surfactant-modified zeolite	298	6.85	15.68	(71)
Zeolite-AC macro-composite	298	7.0	0.190	(72)

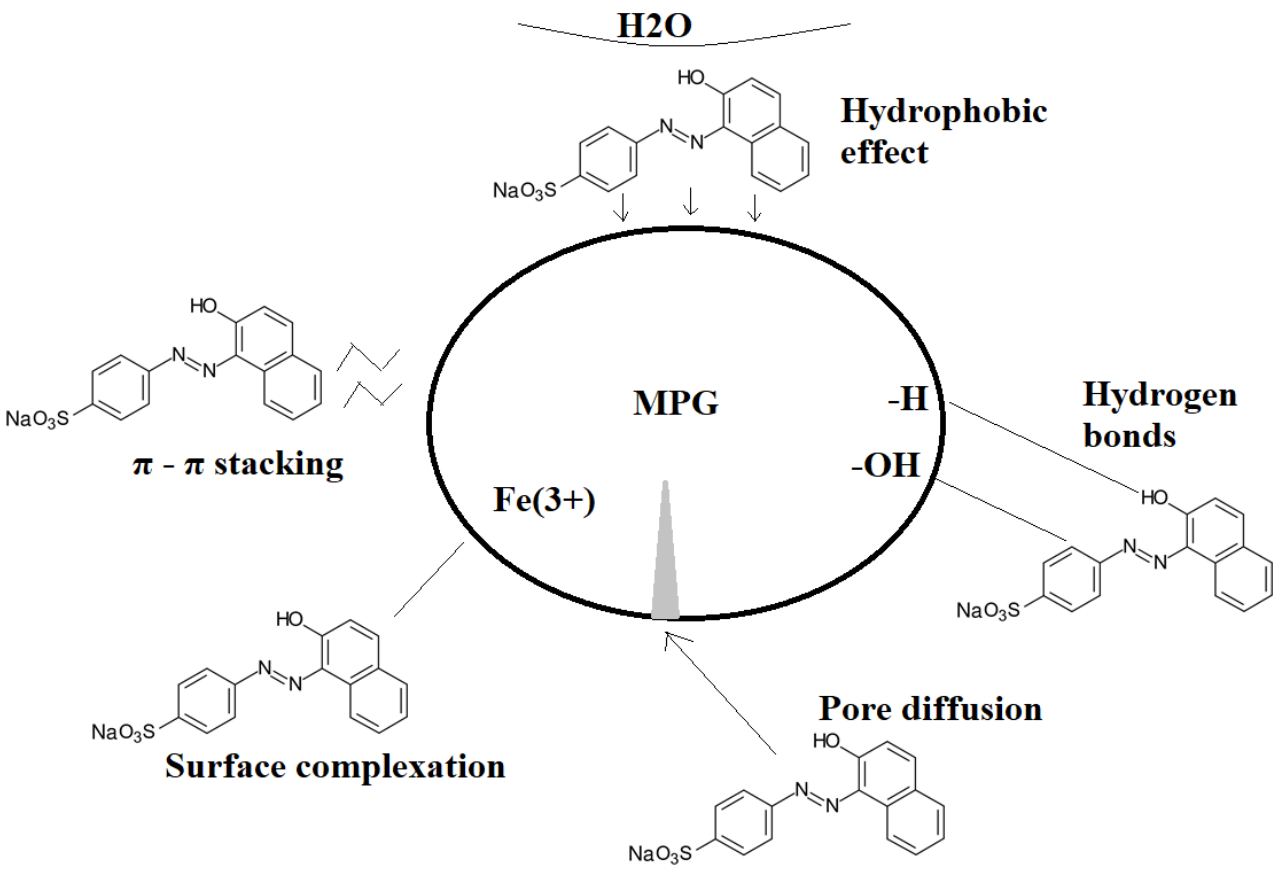

Figure 9: Summary of possible ACO7 adsorption.

Reuse Performance of MPG

The used MPG was regenerated as described by Erdem *et al.* (37) (*see Supplementary*). The ACO7 uptake capacity by the regenerated MPG for 8 cycles was shown in Figure 10. It can be observed that the ACO7 uptake capacity decreases moderately with the increase of cycle times from 90.13 mg/g for the fresh MPG to 83.17 mg/g for the 8 cycles. Therefore, these results still show that there was no clear deterioration observed for the regenerated MPG. It can be surmised that the MPG has excellent reusability potential with only an 8% drop in performance after 8 cycles. The ease of desorption and reuse could be due to the physical nature of interaction between the adsorbent and the adsorbate (73). Physical adsorption forces are not as strong as chemical bonds and are easily broken by the eluents (74).

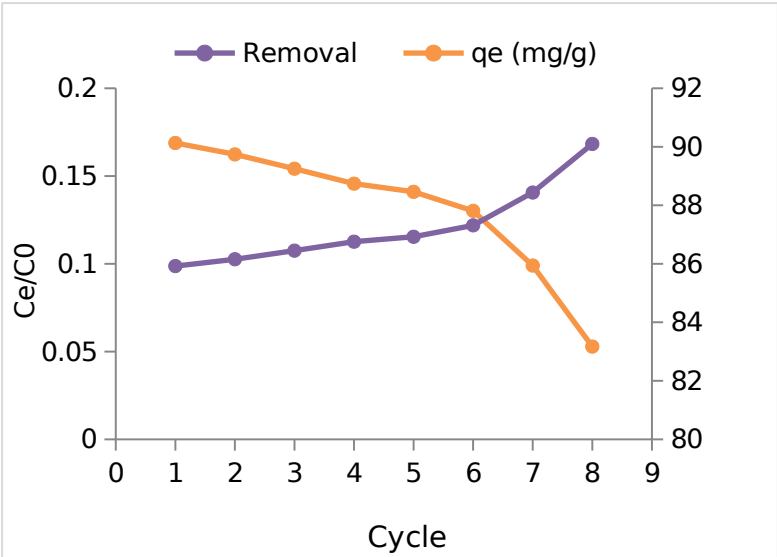

Figure 10: Comparison of ACO7 uptake capacity by fresh and regenerated MPG.

CONCLUSION

The adsorption of ACO7 by mesoporous goethite (MPG) was investigated. The BET specific surface area of MPG was 194.35 m^2/g. The adsorbent was heterogeneous, porous and crystalline in nature. Optimal condition for the adsorption process was 1 g/L adsorbent dosage, temperature of 328 K, pH of 3, 75 minutes' contact time and ACO7 concentration: 100 mg/L which yielded a removal efficiency of 90.13%. The uptake increased with increasing temperature and decreasing pH. The study revealed that intra-particle diffusion and Langmuir model were the best-fit kinetics and isotherm models to describe the process. The uptake of ACO7 by MPG was an endothermic and spontaneous process. The monolayer adsorption capacity of ACO7 onto MPG is 117.9 mg/g (at 328 K). Upon comparison with other adsorbents for ACO7 uptake, MPG has displayed an intermediate adsorption capacity. The major mechanisms for ACO7 uptake onto MPG were pore diffusion, hydrophobic, hydrogen bonds, π – π stacking, and interactions. MPG has excellent reusability potential with only an 8% drop in performance after 8 cycles. For future work, it will be interesting to investigate the mechanistic modeling via statistical physics techniques. The investigation could also be explored in column set-up to know its performance in industrial application scenarios.

REFERENCES

1. Arami M, Yousefi N, Mahmoodi NM. Evaluation of the adsorption kinetics and equilibrium for the potential removal of acid dyes using a biosorbent. Chem Eng J. 2008;139:2-10.

2. Moussavi GR, Mahmoudi M. Removal of azo and anthraquinone reactive dyes from industrial wastewaters using MgO nanoparticles. J Hazard Mater. 2009;168:806–12.

3. Balarak D, Zafariyan M, Igwegbe CA, Onyechi KK and Ighalo JO. Adsorption of Acid Blue 92 Dye from Aqueous Solutions by Single-Walled Carbon Nanotubes: Isothermal, Kinetic, and Thermodynamic Studies. Environmental Processes. 2021: 1-20.

4. Muthukumaran C, Sivakumar VM, Thirumarimurugan M. Adsorption isotherms and kinetic studies of crystal violet dye removal from aqueous solution using surfactant modified magnetic nanoadsorbent. Journal of the Taiwan Institute of Chemical Engineers. 2016;63:354-62.

5. Igwegbe CA, Mohmmadi L, Ahmadi S, Rahdar A, Khadkhodaiy D, Dehghani R, Rahdar S. Modeling of adsorption of Methylene blue dye on Ho-CaWO4 nanoparticles using Response surface methodology (RSM) and Artificial neural network (ANN) techniques. MethodsX. 2019;6:1779-97.

6. Eren E, Cubuk O, Ciftci H, Eren B, Caglar B. Adsorption of basic dye from aqueous solutions by modified sepiolite: equilibrium, kinetics and thermodynamics study. Desalination. 2010;252(1-3):88-96.

7. Özcan A, Özcan AS. Adsorption of Acid Red 57 from aqueous solutions onto surfactant-modified sepiolite. Journal of Hazardous Materials. 2005;125(1-3):252-9.

8. Ahmadi S, Mohammadi L, Rahdar A, Rahdar S, Dehghani R, Igwegbe CA, Kyzas GZ. Acid Dye Removal from Aqueous Solution by Using Neodymium (III) Oxide Nanoadsorbents. Nanomaterials. 2020;10(3):556.

9. Uddin MT, Rukanuzzaman M, Khan MMR, Islam MA. Adsorption of methylene blue from aqueous solution by jackfruit (Artocarpus heteropyllus) leaf powder: A fixed-bed column study. Journal of environmental management. 2009;90(11):3443-50.

10. Hevira L, Zilfa, Rahmayeni, Ighalo JO, Zein R. Biosorption of Indigo Carmine from Aqueous Solution by Terminalia Catappa Shell. Journal of Environmental Chemical Engineering. 2020;8(5):104290.

11. Ighalo JO, Adeniyi AG, Oke EO, Adewiye LT, Motolani FO. Evaluation of Luffa Cylindrica Fibers in A Biomass Packed Bed for The Treatment of Paint Industry Effluent Before Environmental Release. European Journal of Sustainable Development Research. 2020;4(4).

12. Pavan FA, Lima EC, Dias SL, Mazzocato AC. Methylene blue biosorption from aqueous solutions by yellow passion fruit waste. Journal of hazardous materials. 2008;150(3):703-12.

13. Assadi A, Soudavari A, Mohammadian M. Comparison of electrocoagulation and chemical coagulation processes in removing reactive red 196 from aqueous solution. Journal of Human, Environment and Health Promotion. 2016;1(3):172-82.

14. Deniz F, Karaman S. Removal of Basic Red 46 dye from aqueous solution by pine tree leaves. Chemical Engineering Journal. 2011;170(1):67-74.

15. Akazdam S, Chafi M, Yassine W, Gourich B. Removal of acid orange 7 dye from aqueous solution using the exchange resin amberlite FPA-98 as an efficient adsorbent: kinetics, isotherms, and thermodynamics study. Journal of Materials and Environmental Sciences. 2017;8(8):2993-3012.

16. Tatarchuk T, Paliychuk N, Bitra RB, Shyichuk A, Naushad M, Mironyuk I, et al. Adsorptive removal of toxic Methylene Blue and Acid Orange 7 dyes from aqueous medium using cobalt-zinc ferrite

nanoadsorbents. Desalin Water Treat. 2019;150:374-85.

17. Thirunavukkarasu A, Nithya R. Adsorption of acid orange 7 using green synthesized CaO/CeO2 composite: An insight into kinetics, equilibrium, thermodynamics, mass transfer and statistical models. Journal of the Taiwan Institute of Chemical Engineers. 2020.

18. Yousuf M, Mollah A, Gomes J, Das KK, Cocke DL. Electrochemical Treatment of OrangeII Dye Solution-use of Aluminum Sacrificial Electrodes and Floc Characterization. J Hazard Mater. 2010;174:851-8.

19. Uddin MT, Islam MA, Mahmud S, Rukanuzzaman M. Adsorptive removal of methylene blue by tea waste. Journal of Hazardous Materials. 2009;164(1):53-60.

20. Gao H, Zhao S, Cheng X, Wang X, Zheng L. Removal of anionic azo dyes from aqueous solution using magnetic polymer multi-wall carbon nanotube nanocomposite as adsorbent. Chemical Engineering Journal. 2013;223:84-90.

21. Ighalo JO, Igwegbe CA, Aniagor CO, Oba SN. A Review of Methods for the Removal of Penicillins from Water. Journal of Water Process Engineering, 2021;39:101886.

22. Balarak D, Jaafari J, Hassani G, Mahdavi Y, Tyagi I, Agarwal S, Gupta VK. The use of low-cost adsorbent (Canola residues) for the adsorption of methylene blue from aqueous solution: Isotherm, kinetic and thermodynamic studies. Colloids and Interface Science Communications. 2015;7:16-9.

23. Bayram T, Bucak S, Ozturk D. BR13 dye removal using Sodium Dodecyl Sulfate modified montmorillonite: Equilibrium, Thermodynamic, Kinetic and Reusability studies. Chemical Engineering and Processing-Process Intensification, 2020;158:108186.

24. Ozturk D, Sahan T, Bayram T, Erkus A. Application of response surface methodology (RSM) to optimize the adsorption conditions of cationic basic yellow 2 onto pumice samples as a new adsorbent. Fresen. Environ. Bull, 2017,26:3285-5.

25. Ler A, Stanforth R. Evidence for surface precipitation of phosphate on goethite. Environmental Science & Technology. 2003;37(12):2694-700.

26. Zhou Q, Maurice PA, Cabaniss SE. Size fractionation upon adsorption of fulvic acid on goethite: Equilibrium and kinetic studies. Geochimica et Cosmochimica Acta. 2001;65(5):803-12.

27. Xie J, Gu X, Tong F, Zhao Y, Tan Y. Surface complexation modeling of Cr (VI) adsorption at the goethite–water interface. Journal of colloid and interface science. 2015;455:55-62.

28. Foroutan R, Mohammadi R, Adeleye AS, Farjadfard S, Esvandi Z, Arfaeinia H, Sorial GA, Ramavandi B, Sahebi S. Efficient arsenic (V) removal from contaminated water using natural clay and clay composite adsorbents. Environmental Science and Pollution Research. 2019;26(29):29748-62.

29. Dong Y, Yang H, Rao R, Zhang A. Selective synthesis of α-FeOOH and α-Fe2O3 nanorods via a temperature controlled process. Journal of Nanoscience and Nanotechnology. 2009;9(8):4774-9.

30. Ighalo JO, Adeniyi AG, Eletta OAA, Arowoyele LT. Competitive adsorption of Pb(II), Cu(II), Fe(II) and Zn(II) from aqueous media using biochar from oil palm (Elaeis guineensis) fibers: A Kinetic and equilibrium study. Indian Chemical Engineer. 2020:1-11.

31. Igwegbe CA, Onukwuli OD, Ighalo JO, Okoye PU. Adsorption of cationic dyes on Dacryodes edulis seeds activated carbon modified using phosphoric acid and sodium chloride. Environmental Processes. 2020;7(4):1151-71.

32. AbdurRahman FB, Akter M, Abedin MZ. Dyes removal from textile wastewater using orange peels. International journal of scientific & technology research. 2013;2(9):47-50.

33. Li F, Geng D, Cao Q. Adsorption of As (V) on aluminum-, iron-, and manganese-(oxyhydr) oxides: equilibrium and kinetics. Desalination and Water Treatment. 2015;56(7):1829-38.

34. Ighalo JO, Adeniyi AG. A Mini-Review of the Morphological Properties of Biosorbents Derived from Plant Leaves. SN Applied Sciences. 2020;2(3):509.

35. Ighalo JO, Adeniyi AG, Adelodun AA. Recent Advances on the Adsorption of Herbicides and Pesticides from Polluted Waters: Performance Evaluation via Physical Attributes. Journal of Industrial and Engineering Chemistry. 2020.

36. Özcan AS, Erdem B, Özcan A. Adsorption of Acid Blue 193 from aqueous solutions onto Na–bentonite and DTMA–bentonite. Journal of colloid and Interface science. 2004;280(1):44-54.

37. Erdem B, Özcan AS, Özcan A. Preparation of HDTMA-bentonite: Characterization studies and its adsorption behavior toward dibenzofuran. Surface and Interface Analysis. 2010;42(6-7):1351-6.

38. Özcan A, Ömeroğlu Ç, Erdoğan Y, Özcan AS. Modification of bentonite with a cationic surfactant: an adsorption study of textile dye Reactive Blue 19. Journal of hazardous materials. 2007;140(1-2):173-9.

39. Zhou Y, Jin X-Y, Lin H, Chen Z-L. Synthesis, characterization and potential application of organobentonite in removing 2, 4-DCP from industrial wastewater. Chemical engineering journal. 2011;166(1):176-83.

40. Şahan T, Öztürk D. Investigation of Pb (II) adsorption onto pumice samples: application of optimization method based on fractional factorial design and response surface methodology. Clean Technologies and Environmental Policy, 2014;16(5):819-831.

41. Mittal A, Krishnan L, Gupta V. Removal and recovery of malachite green from wastewater using an agricultural waste material, de-oiled soya. Separation and Purification Technology, 2005;43(2): 125-133.

42. Zazouli MA, Yazdani J, Balarak D, Ebrahimi M, Mahdavi Y. Removal Acid Blue 113 from aqueous solution by canola. J Mazandaran Univ Med Sci 2013;22(2):71-8.

43. Luo P, Zhao Y, Zhang B, Liu J, Yang Y, Liu J. Study on the adsorption of Neutral Red from aqueous solution onto halloysite nanotubes. Water research. 2010;44(5):1489-97.

44. Pekkuz H, Uzun I, Güzel F. Kinetics and thermodynamics of the adsorption of some dyestuffs from aqueous solution by poplar sawdust. Bioresource technology. 2008;99(6):2009-17.

45. Eletta OAA, Adeniyi AG, Ighalo JO, Onifade DV, Ayandele FO. Valorisation of Cocoa (Theobroma cacao) Pod Husk as Precursors for the Production of Adsorbents for Water Treatment. Environmental Technology Reviews. 2020;9(1):20-36.

46. Igwegbe CA, Oba SN, Aniagor CO, Adeniyi AG, Ighalo JO. Adsorption of Ciprofloxacin from Water: A Comprehensive Review. Journal of Industrial and Engineering Chemistry. 2020.

47. Baocheng Q, Jiti Z, Xiang X, Zheng C, Hongxia Z, Xiaobai Z. Adsorption behavior of Azo Dye CI Acid Red 14 in aqueous solution on surface soils. Journal of Environmental Sciences. 2008;20(6):704-9.

48. Langmuir I. The adsorption of gases on plane surfaces of glass, mica and platinum. Journal of the American Chemical society. 1918;40(9):1361-403.

49. Freundlich H. Over the adsorption in solution. J Phys Chem. 1906;57(385471):1100-7.

50. Temkin M, Pyzhev V. Recent modifications to Langmuir isotherms. Acta Physiochim URSS. 1940;12:217-22.

51. Dubinin MM, Radushkevich LV. Equation of the characteristic curve of activated charcoal. Proceedings of the Academy Sciences Physical Chemistry Section, USSR. 1947;55:331-3.

52. Gök Ö, Özcan AS, Özcan A. Adsorption behavior of a textile dye of Reactive Blue 19 from aqueous solutions onto modified bentonite. Applied surface science. 2010;256(17):5439-43.

53. Lagergren S, Svenska BK. On the theory of so-called adsorption of dissolved substances. The Royal Swedish Academy of Sciences Documents Band. 1898;24:1-13.

54. Ho YS, McKay G. Pseudo-second order model for sorption processes. Process Biochemistry. 1999;34:451–65.

55. Weber W, Morris J. Kinetics of adsorption on carbon from solution. J Sanit Eng Div Am Soc Civ Eng 1963;89:31-60.

56. Moussavi SP, MohammadianFazli M. Acid violet 17 Dye decolorization by multi-walled carbon nanotubes from aqueous solution. Journal of Human, Environment and Health Promotion. 2016;1(2):110-7.

57. Mohamed MM. Acid dye removal: comparison of surfactant-modified mesoporous FSM-16 with activated carbon derived from rice husk. Journal of Colloid and Interface Science. 2004;272(1):28-34.

58. Balarak D, Mostafapour FK. Adsorption of acid red 66 dye from aqueous solution by heat-treated rice husk. Research Journal of Chemistry and Environment. 2018;22(12):80-4.

59. Ighalo JO, Ajala JO, Umunweke G, Ogunniyi S, Adeyanju CA, Igwegbe CA, Adeniyi AG. Mitigation of Clofibric Acid Pollution by Adsorption: A Review of Recent Developments. Journal of Environmental Chemical Engineering. 2020;8(5):104264.

60. Inyinbor A, Adekola F, Olatunji GA. Kinetics, isotherms and thermodynamic modeling of liquid phase adsorption of Rhodamine B dye onto Raphia hookerie fruit epicarp. Water Resources and Industry. 2016;15:14-27.

61. Kuo CY, Wu CH, Wu JY. Adsorption of direct dyes from aqueous solutions by carbon nanotubes: Determination of equilibrium, kinetics and thermodynamics parameters. J Colloid Interface Sci. 2008;327(2):308–15.

62. Balarak D, Chandrika K, Igwegbe CA, Ahmadi S, Umembamalu CJ. Biosorption of phenol using modified barley husk: studies on equilibrium isotherm, kinetics, and thermodynamics of interactions. Sigma: Journal of Engineering & Natural Sciences/Mühendislik ve Fen Bilimleri Dergisi. 2020;38(3).

63. Eletta AAO, Tijani IO, Ighalo JO. Adsorption of Pb(II) and Phenol from Wastewater Using Silver Nitrate Modified Activated Carbon from Groundnut (Arachis hypogaea L.) Shells. West Indian Journal of Engineering. 2020;43(1):26-35.

64. Jung K-W, Choi BH, Hwang M-J, Jeong T-U, Ahn K-H. Fabrication of granular activated carbons derived from spent coffee grounds by entrapment in calcium alginate beads for adsorption of acid orange 7 and methylene blue. Bioresource Technology. 2016;219:185-95.

65. Yoon S, Calvo JJ, So MC. Removal of acid orange 7 from aqueous solution by metal-organic frameworks. Crystals. 2019;9(1):17.

66. Pan X, Zhang M, Liu H, Ouyang S, Ding N, Zhang P. Adsorption behavior and mechanism of acid orange 7 and methylene blue on self-assembled three-dimensional MgAl layered double hydroxide: Experimental and DFT investigation. Applied Surface Science. 2020:146370.

67. Jia L, Liu W, Cao J, Wu Z, Yang C. Modified multi-walled carbon nanotubes assisted foam fractionation for effective removal of acid orange 7 from the dyestuff wastewater. Journal of Environmental Management. 2020;262:110260.

68. Saeidi M, Biglari H, Rahdar S, Baneshi M, Ahamadabadi M, Narooie MR, et al. The adsorptive acid orange 7 using Kenya tea pulps ash from aqueous environments. Journal of Global Pharma Technology. 2017;9(4):13-9.

69. Nourmoradi H, Ghiasvand AR, Noorimotlagh Z. Removal of methylene blue and acid orange 7 from aqueous solutions by activated carbon coated with zinc oxide (ZnO) nanoparticles: equilibrium, kinetic, and thermodynamic study. Desalination and Water Treatment. 2014;55(1):252–62.

70. Silva JP, Sousa S, Rodrigues J, Antunes H, Porter JJ, Gonçalves I, et al. Adsorption of acid orange 7 dye in aqueous solutions by spent brewery grains. Separation and Purification Technology. 2004;40(3):309-15.

71. Jin X, Jiang M, Shan X, Pei Z, Chen Z. Adsorption of methylene blue and orange II onto unmodified and surfactant-modified zeolite. Journal of Colloid and Interface Science. 2008;328(2):243–7.

72. Lim CK, Bay HH, Neoh CH, Aris A, Majid ZA, Ibrahim Z. Application of zeolite-activated carbon macrocomposite for the adsorption of Acid Orange 7: isotherm, kinetic and thermodynamic studies. Environmental Science and Pollution Research. 2013;20(10):7243-55.

73. Hevira L, Zilfa, Rahmayeni, Ighalo JO, Aziz H, Zein R. Terminalia catappa shell as low-cost biosorbent for the removal of methylene blue from aqueous solutions. Journal of Industrial and Engineering Chemistry, 2021.

74. Ighalo JO, Igwegbe CA, Adeniyi AG, Adeyanju CA, and Ogunniyi S, Mitigation of Metronidazole (Flagyl) Pollution in Aqueous Media by Adsorption: A Review. Environmental Technology Reviews, 2020; 9(1):137-148.

Ultimate Eradication of Acid Orange 7 from Contaminated Liquid via Synthesized Mesoporous Goethite

Davoud Balarak, Fatemeh Ganji, Periakaruppan Rajiv, Chinenye Adaobi Igwegbe*, Joshua O. Ighalo

SUPPLEMENTARY INFORMATION

MPG preparation

The mesoporous goethite was synthesized by the oxidation of ferrous sulfate heptahydrate with hydrogen peroxide in aqueous solution following the method reported by Dong et al. (2009). Typically, 0.70 g ferrous sulfate heptahydrate were added to 21.0 g ultrapure water, and then 30% hydrogen peroxide (6.0 mL) was added to the above-mentioned solution under vigorous stirring to obtain a homogeneous yellow slurry solution. Then the suspension was transferred into a PTFE lined hydrothermal synthesis reactor maintaining 150 °C for 6 h. At last, the solid product was centrifuged and rinsed with ultrapure water for several times until the supernatant was near neutral and dried overnight at 80 °C under vacuum.

Regeneration of used MPG

In this study, the used MPG was regenerated by NaCl solution (1 M) treatment, since the “NaCl regeneration” method stood out in all methods (Erdem et al. 2010). In the regeneration process, the used MPG was mixed with 1 M NaCl solution. Then, the mixture was stirred at 200 rpm at 25 °C for 2 h and the regeneration was performed 8 steps. Finally, the solid samples were filtered, washed, dried and sieved through a 100 mesh for further analysis. And comparison was made between the AO7 uptake capacity obtained using regenerated samples and with those obtained using fresh MPG ones.